AD-A083 555 NAVAL UNDERWATER SYSTEMS CENTER NEW LONDON CT NEW LO--ETC F/G 17/1
A NEARFIELD MODEL OF THE PARAMETRIC RADIATOR PART II. SATURATED--ETC(U)
MAY 76 R H MELLEN
UNCLASSIFIED NUSC-TM-PA4-53-76 NL

1 OF 1
AD A
083555

END
DATE
FILMED
5-80
DTIC

TM No.
PA4-53-76

NAVAL UNDERWATER SYSTEMS CENTER
NEW LONDON LABORATORY
NEW LONDON, CONNECTICUT 06320

Technical Memorandum

A NEARFIELD MODEL OF THE PARAMETRIC RADIATOR
PART II. SATURATED SOURCE LEVELS.*

17 May 1976

Prepared by: R H Mellen
R. H. Mellen
Plans and Analysis Directorate

*To be presented at the 7th International Symposium on Nonlinear Acoustics, Virginia Polytechnic University, Blacksburg, VA, August 1976.

Reverse Blank

TM No.
PA4-53-76

ABSTRACT

In the nearfield model of the parametric radiator, source levels were obtained by assuming the primary wave to be plane-cylindrical or diverging-conical, depending on whether the observation range was less or greater than the Rayleigh distance. The two cases are now combined by means of the "horn" model, which approximates primary wave diffraction for a piston source. Saturation effects are also incorporated by means of a nonlinear attenuation approximation.

ADMINISTRATIVE INFORMATION

This memorandum was prepared under NUSC Project A61415, "Parametric Sonar Echo Ranging Systems," Principal Investigator W. L. Konrad and Program Manager J. Neely, NAVSEA Code 06H1.

The author of this memorandum is located at the New London Laboratory, Naval Underwater Systems Center, New London, CT 06320.

INTRODUCTION

In reference (1), a complex contour integration method was used to calculate nearfield parametric source levels for two primary wave models: a plane-wave cylindrically collimated source for ranges less than the Rayleigh distance and a spherical wave conically collimated source for greater ranges. The two cases are now combined by means of the horn model and the effects of saturation are included by means of a nonlinear taper approximation.

HORN MODEL

In the horn model of Fig. 1, we require that the primary wave be predominantly plane near the source and predominantly spherical for ranges much greater than the Rayleigh distance R_o. The cross-sectional area of the horn is chosen to maintain constant source density per-unit-length when attenuation is neglected. On the axis, the primary peak pressure is approximated as

$$P = \mathrm{Re}\,\frac{P_o}{1 + \rho i} \sum_{n=1}^{2} \exp\,(i\omega_n \tau) \qquad (1)$$

where P_o is the initial pressure of each component, τ is the retarded time and $\rho = r/R_o$ is the scaled distance from the piston source.

Squaring Eq. (1) and taking the cross-sectional area as $S = S_o\,(1 + \rho^2)$ we can write the dimensionless normalized source density per-unit-length as

$$\left| \frac{P^2\, S}{P_o^2\, S_o} \right| = 2\,\frac{[\overline{\sin^2(\Omega\tau)} + \rho^2\,\overline{\cos^2(\Omega\tau)}]}{1 + \rho^2} \equiv 1 \qquad (2)$$

where S_o is the piston area, $\Omega = (\omega_1 + \omega_2)/2$ and the bars indicate the average value. The $\sin^2(\Omega\tau)$ term is taken as the cylindrical component of the source density and the $\cos^2(\Omega\tau)$ term as the conical component.

The parametric source strength relative to the Westervelt source strength at infinite range can then be written symbolically as

$$Y = \int_0^{\infty} \frac{dY_1}{1+\rho^2} + \int_0^{\infty} \frac{\rho^2 \, dY_2}{1+\rho^2} \tag{3}$$

where Y_1 and Y_2 are Eq. (9) and Eq. (12) of reference (1), respectively.

SATURATION TAPER

Reference (2) gives the derivation of a nonlinear taper function as

$$T^2(r) = \frac{2}{K^2}\left[\frac{1+K}{\sqrt{1+2K}} - 1 \right], \quad K = 3\left(\frac{\sigma(r)}{2\pi}\right)^2 \tag{4}$$

where $\sigma(r)$ is the fictitious nonlinear phase distortion angle at the peak envelope of the primary wave. For $\sigma > 1$, the waveform becomes multivalued and the jump approximation is used to restore continuity at the shock front. Interaction effects of absorption are ignored and the linear and nonlinear attenuations are multiplicative.

The phase distortion angle is taken as the magnitude

$$\sigma(r) = \frac{\beta k_o}{\rho_o c_o^2} \int_0^r |P(r')| \, dr' \tag{5}$$

where β is the nonlinearity number and $|P(r')|$ is the peak envelope pressure of Eq. (1). Equation (5) becomes

$$\sigma(\rho) = 2X \int_0^{\rho} \frac{d\rho'}{\sqrt{1+\rho'^2}} = 2X \sinh^{-1}(\rho) \tag{6}$$

where $X = \beta P_o k_o R_o / \rho_o c_o^2$ is the saturation number.

Equation (3) then becomes

$$Y = \int_0^{\infty} \frac{dY_1 T^2(\rho)}{1+\rho^2} + \int_0^{\infty} \frac{dY_2 \rho^2 T^2(\rho)}{1+\rho^2} = \hat{Y}_1 + \hat{Y}_2 \tag{7}$$

COMBINED MODEL

For the cylindrical component Eq. (9) of reference (1) can be written

$$Y_1 = \frac{1}{i v_1} \int_0^{u_o} dt\, e^{-t} - \frac{1}{2} \exp(-i v_1) \int_0^{\infty} dt\, e^{-t} \left[1 - \frac{z_1}{\sqrt{z_1^2 + B_1^2}} \right] \tag{8}$$

where L is the range from the origin to the field point, $u_o = 2\alpha L$, $t = 2\alpha r$, $t_o = 2\alpha R_o$, $v_1 = t_o k/k_o u_o$, $B_1^2 = 4 i u_o v_1$, and $z_1 = t - u_o + i v_1$. The second integrand of Eq. (8) involved a change to the complex variable $z = 2\alpha x + i k \left(\sqrt{a^2 + x^2} + x\right)$ where $x = r - L$ and a change of contour to one of constant imaginary value. In Eq. (6) and Eq. (7), the corresponding variable ρ becomes complex and we have

$$\hat{Y}_1 = \frac{u_o k}{i t_o k_o} \left[\int_0^{u_o} \frac{dt\, e^{-t} T^2(t/t_o)}{1 + (t/t_o)^2} - \frac{1}{2} e^{-i v_1} \int_0^{\infty} \frac{dt\, e^{-t}\left(1 - \frac{z_1}{\sqrt{z_1^2 + B_1^2}}\right) T^2(\zeta_1)}{1 + \zeta_1^2} \right] \tag{9}$$

where $\zeta_1 = \left(z_1 + 2u_o - \sqrt{z_1^2 + B_1^2}\right)/2 t_o$

For the conical component, Eq. (12) of reference (1) can be written

$$Y_2 = \frac{u_o}{i\, v_2} \int_0^{u_o} dt\, \frac{e^{-t}}{t} - \int_0^{\infty} \frac{dt\, e^{-t}\, \left(1 - \frac{z_2}{\sqrt{z_2^2 + B_2^2}}\right)}{z_2 + 2u_o - \sqrt{z_2^2 + B_2^2}} \qquad (10)$$

where $v_2 = u_o\, k/k_o\, t_o$, $B_2^2 = 4i\, u_o\, v_2$ and $z_2 = t - u_o + i\, v_2$. The residue is omitted because the combined solution has no pole.

By similar change of ρ to complex form in Eq. (6) and Eq. (7), we have

$$\hat{Y}_2 = \frac{k}{i\, k_o} \int_0^{u_o} \frac{dt\, e^{-t}\, T^2(t/t_o)}{1 + (t/t_o)^2} - \frac{1}{2} \int_0^{\infty} \frac{dt\, e^{-t}\, \zeta_2 \left(1 - \frac{z_2}{\sqrt{z_2^2 + B_2^2}}\right)}{1 + \zeta_2^2}\, T^2(\zeta_2) \qquad (11)$$

when $\zeta_2 = \left(z_2 + 2u_o - \sqrt{z_2^2 + B_2^2}\right)/2\, t_o$.

Equations (9) and (11) were evaluated numerically as discontinuous functions at $t = u_o$.

RESULTS

Some results are shown in Figs. 2-17 for selected values of the downshift ratio $k_o/k = F_o/F$, the absorption number AR_o(dB) = $8.7\, \alpha\, R_o$, and the saturation parameter X(dB) = 20 $\log_{10} X$. The ordinates are Y(dB) = 20 log $|Y|$ and the abscissas are the scaled range L/R_o . For values of the saturation parameter less than -15 dB, the effects of saturation rapidly become negligible. At long ranges the relative levels approach -20 $\log_{10} X$ dependence when X is large. Since the reference source level (Westervelt) is given by $20 \log_{10} Y_o$ where $Y_o = P_o R_o X(F/F_o)^2/4\alpha R_o$, the actual source levels go from $40 \log_{10} X$ dependence in the unsaturated regime to $20 \log_{10} X$ dependence in the saturated.

The RMS parametric source level may be calculated from the formula

$$SL = SL_o + Y(dB) + X(dB) - 40 \log_{10} (F_o/F) - 20 \log (AR_o) + 6.7 \text{ dB//1}\mu\text{Pa} \cdot \text{m} \quad (12)$$

where SL_o is the RMS source level of each primary component. For 10°C sea water at moderate depth we have from reference (3)

$$X(dB) = SL_o + 20 \log_{10} (F_o/1 \text{ kHz}) - 280.6 \quad (13)$$

where F_o is the mean primary frequency in kHz.

ACKNOWLEDGMENT

Programming for the UNIVAC 1108 Computer was done by Mrs. T. A. Garrett (Code PA41).

REFERENCES

(1) R. H. Mellen, "A Nearfield Model of the Parametric Radiator," NUSC Technical Memorandum No. PA4-230-75, December 1975.

(2) M. B. Moffett and R. H. Mellen, "A Model of Parametric Sources," submitted to Journal of the Acoustical Society of America.

(3) H. M. Merklinger, R. H. Mellen and M. B. Moffett, "Finite Amplitude Losses in Spherical Sound Waves," Journal of the Acoustical Society of America, Vol. 59, 1976, pp. 755-759.

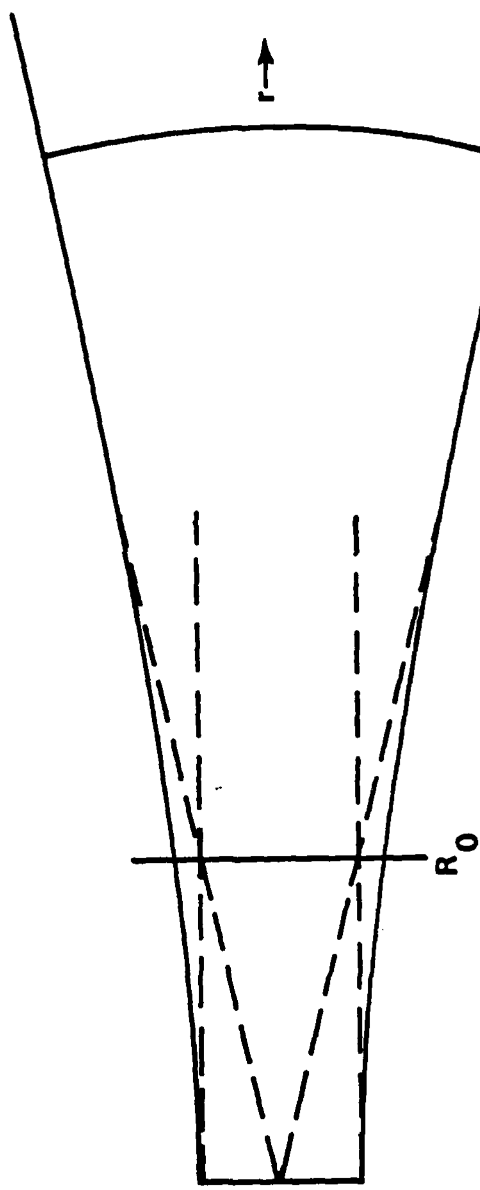

FIG. 1 - HORN MODEL

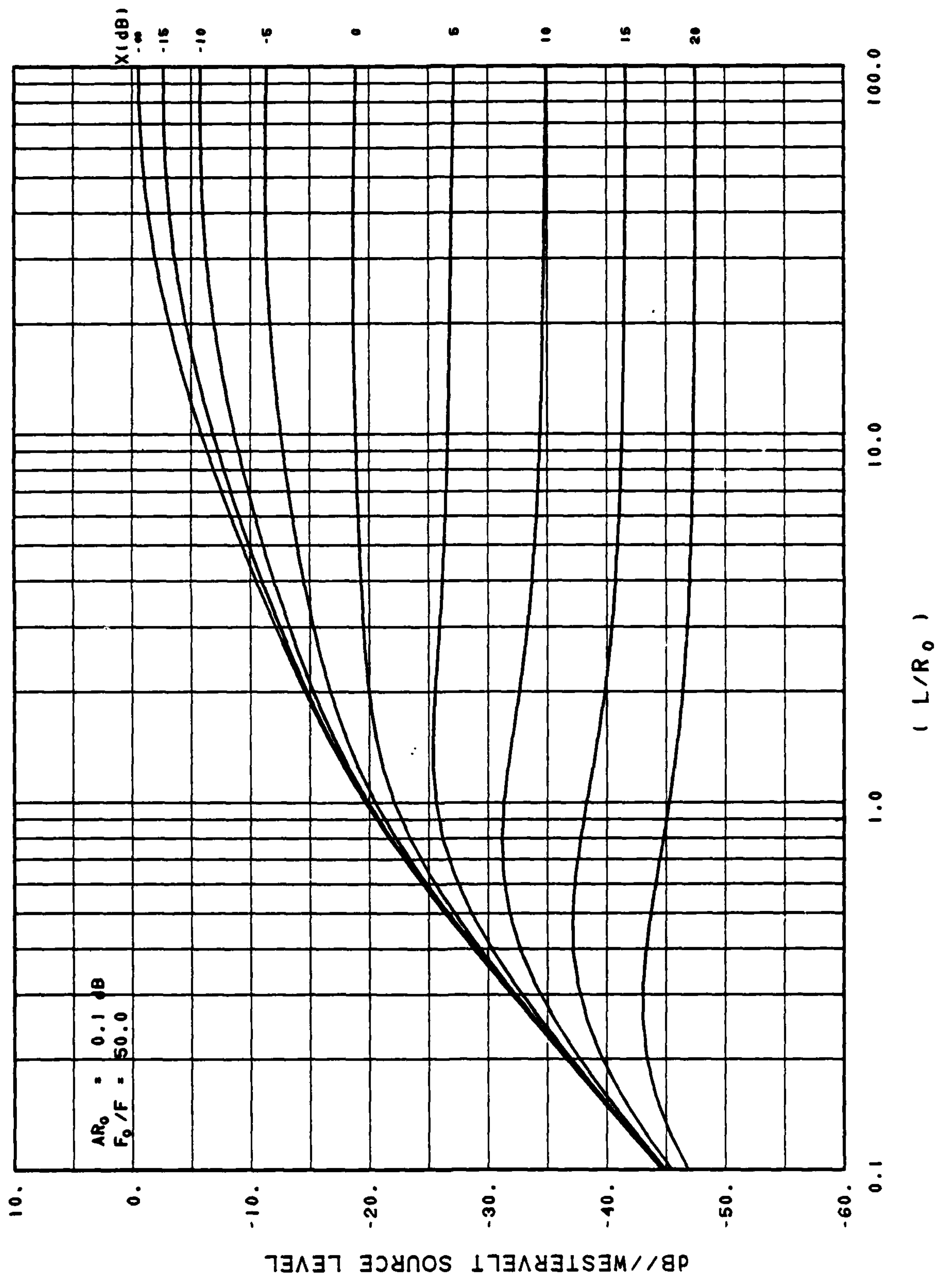

RELATIVE SOURCE LEVEL VS SCALED RANGE

Figure 2

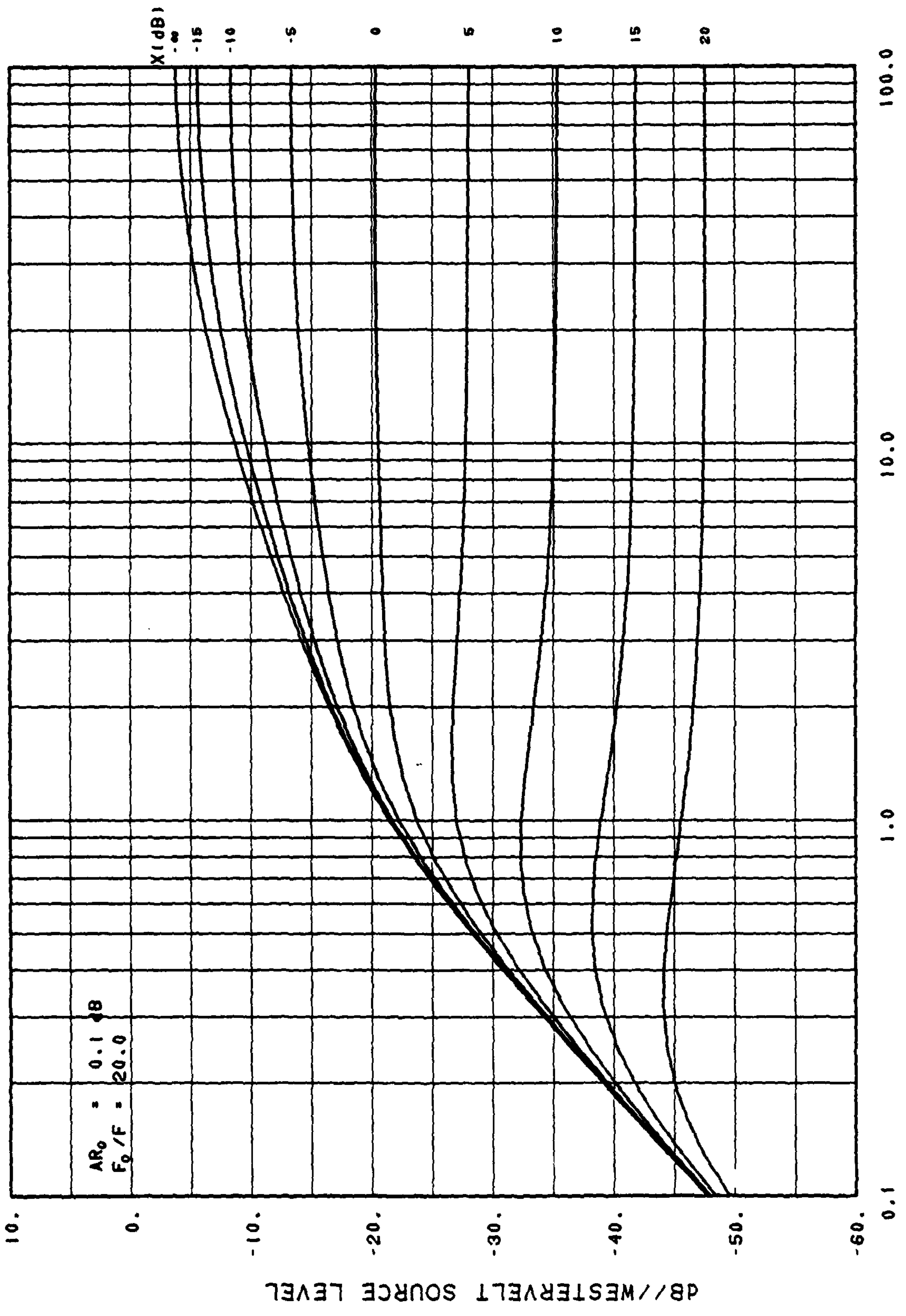

(L/R_o)

RELATIVE SOURCE LEVEL VS SCALED RANGE

Figure 3

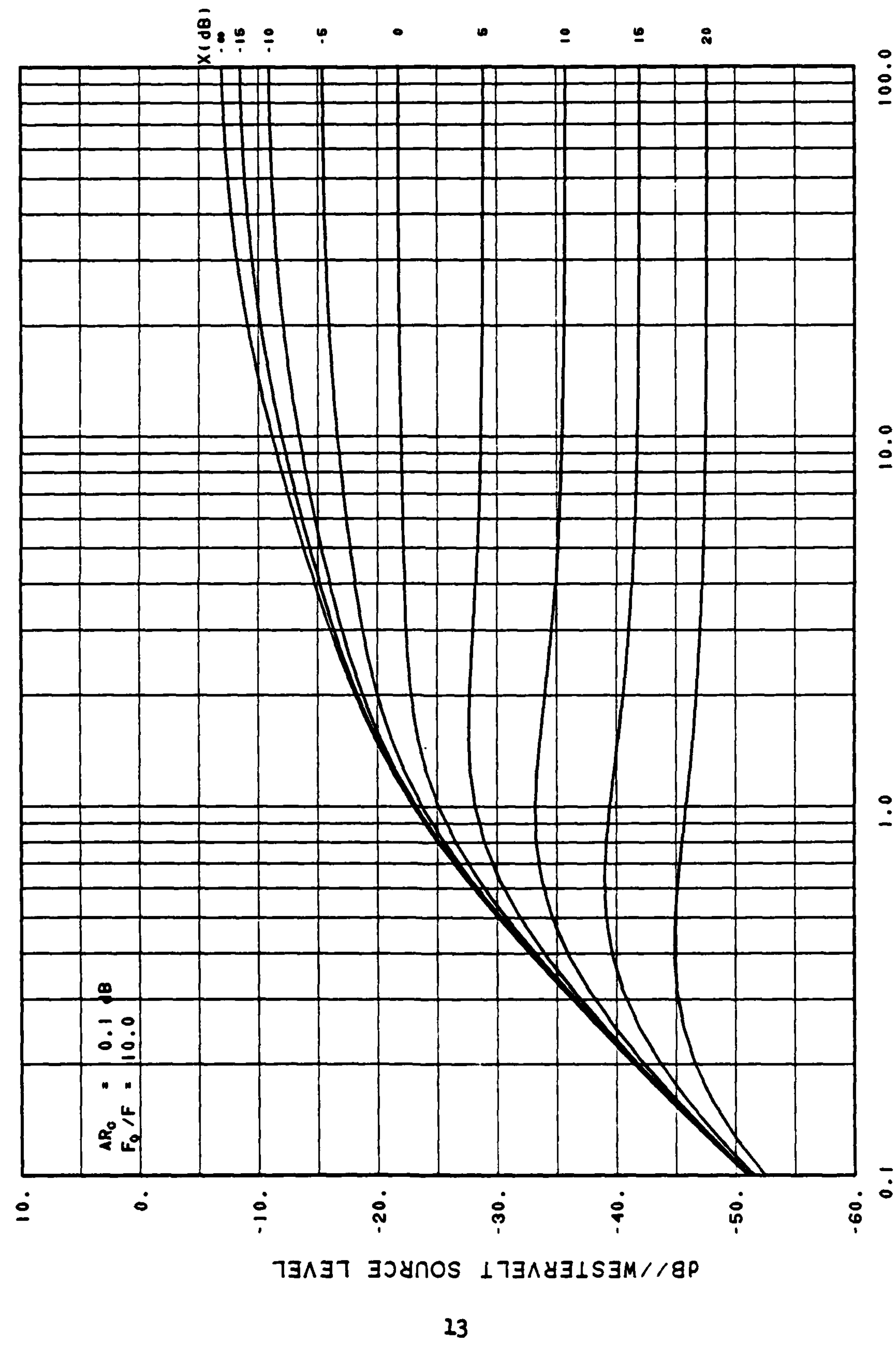

(L/R_0)

RELATIVE SOURCE LEVEL VS SCALED RANGE

Figure 4

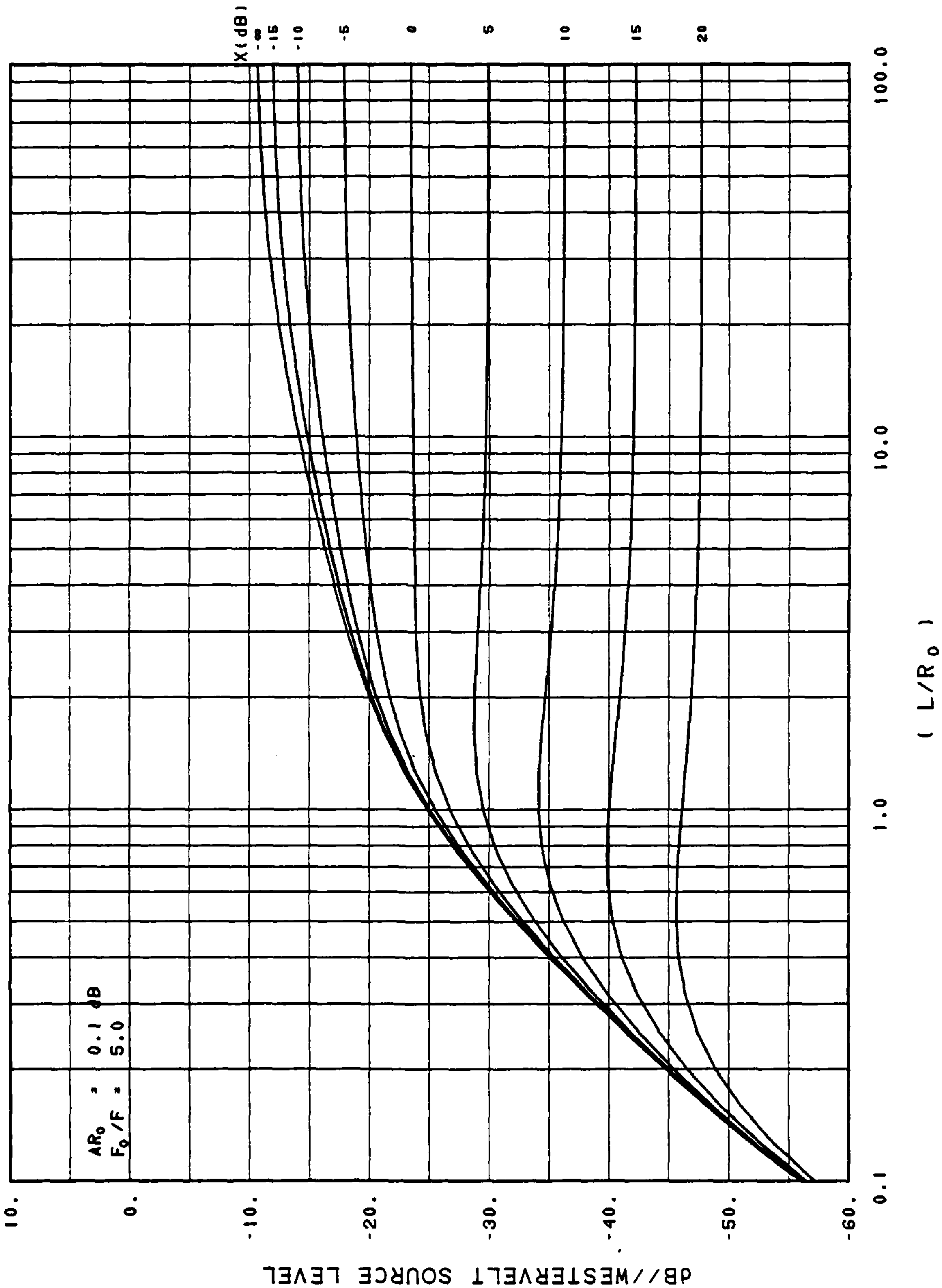

RELATIVE SOURCE LEVEL VS SCALED RANGE

Figure 5

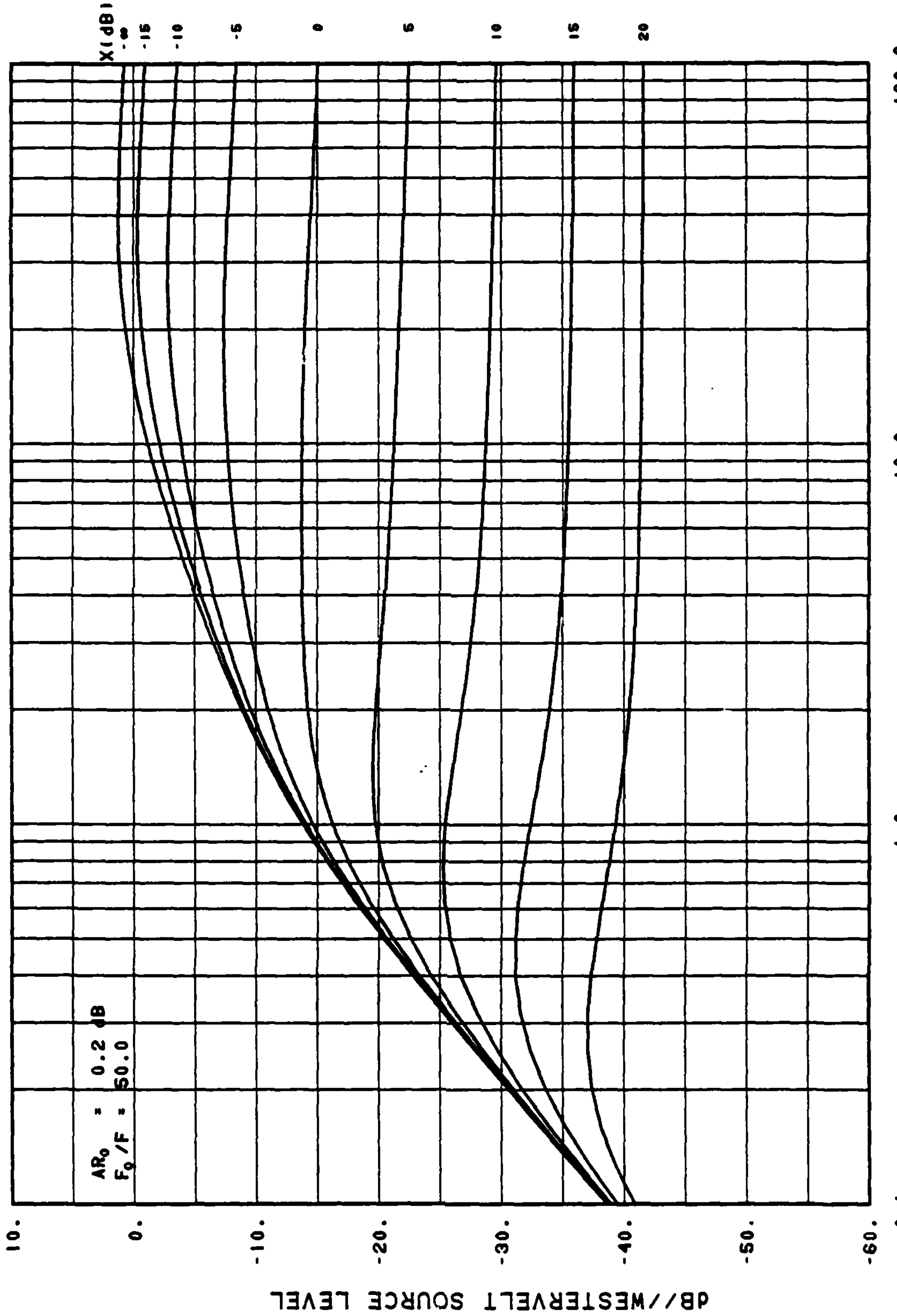

(L/R_0)

RELATIVE SOURCE LEVEL VS SCALED RANGE

Figure 6

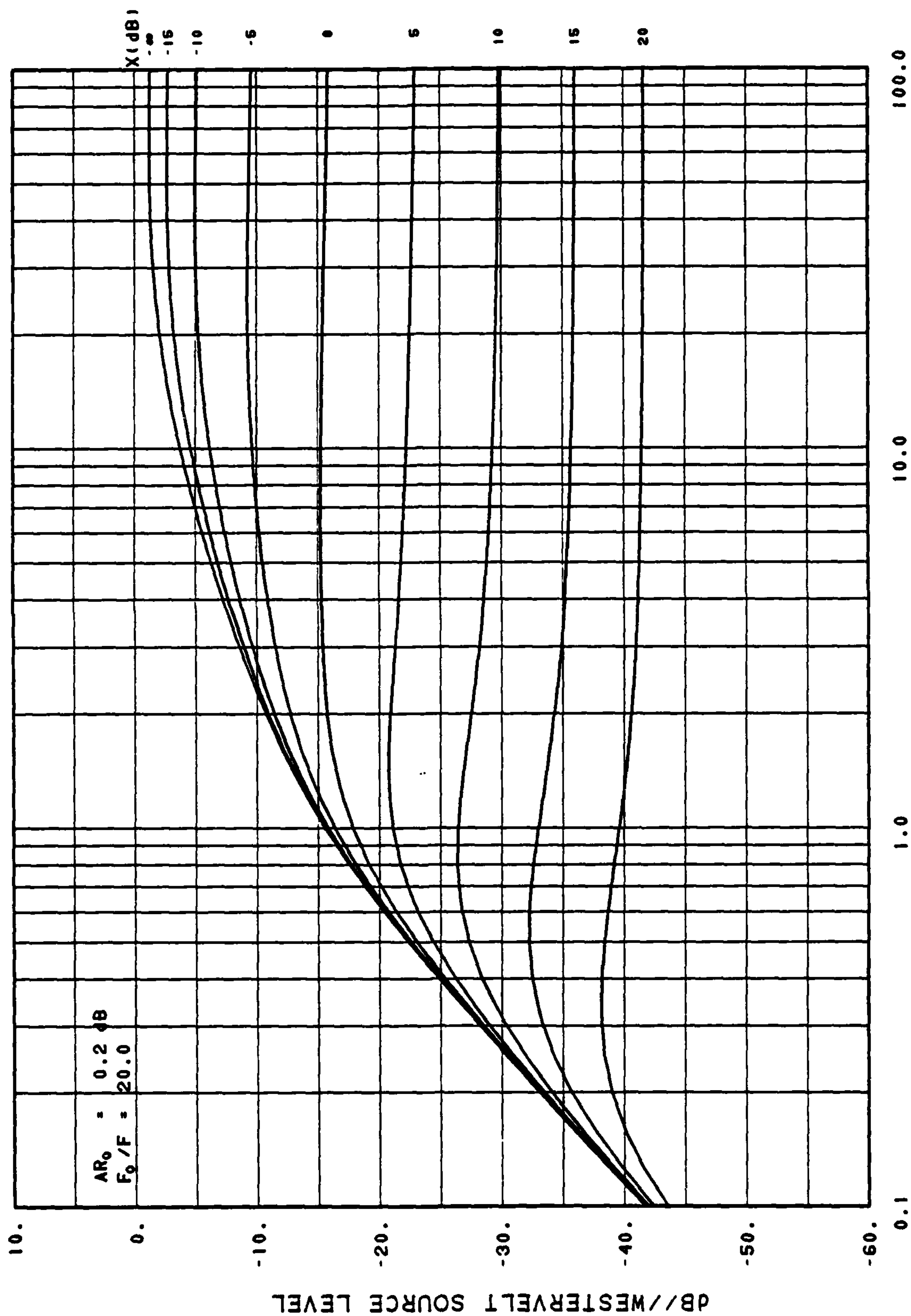

(L/R_0)

RELATIVE SOURCE LEVEL VS SCALED RANGE

Figure 7

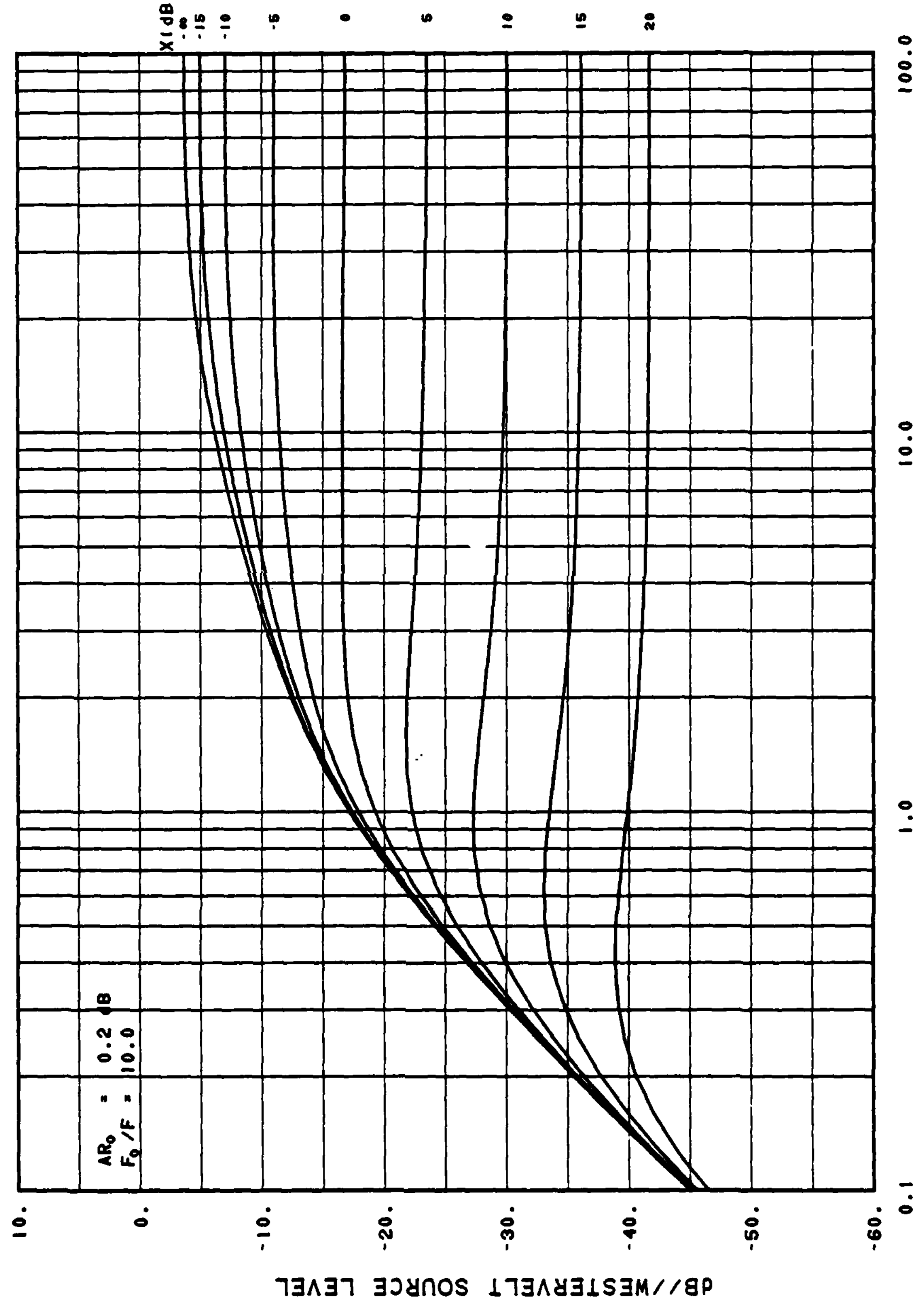

RELATIVE SOURCE LEVEL VS SCALED RANGE

Figure 8

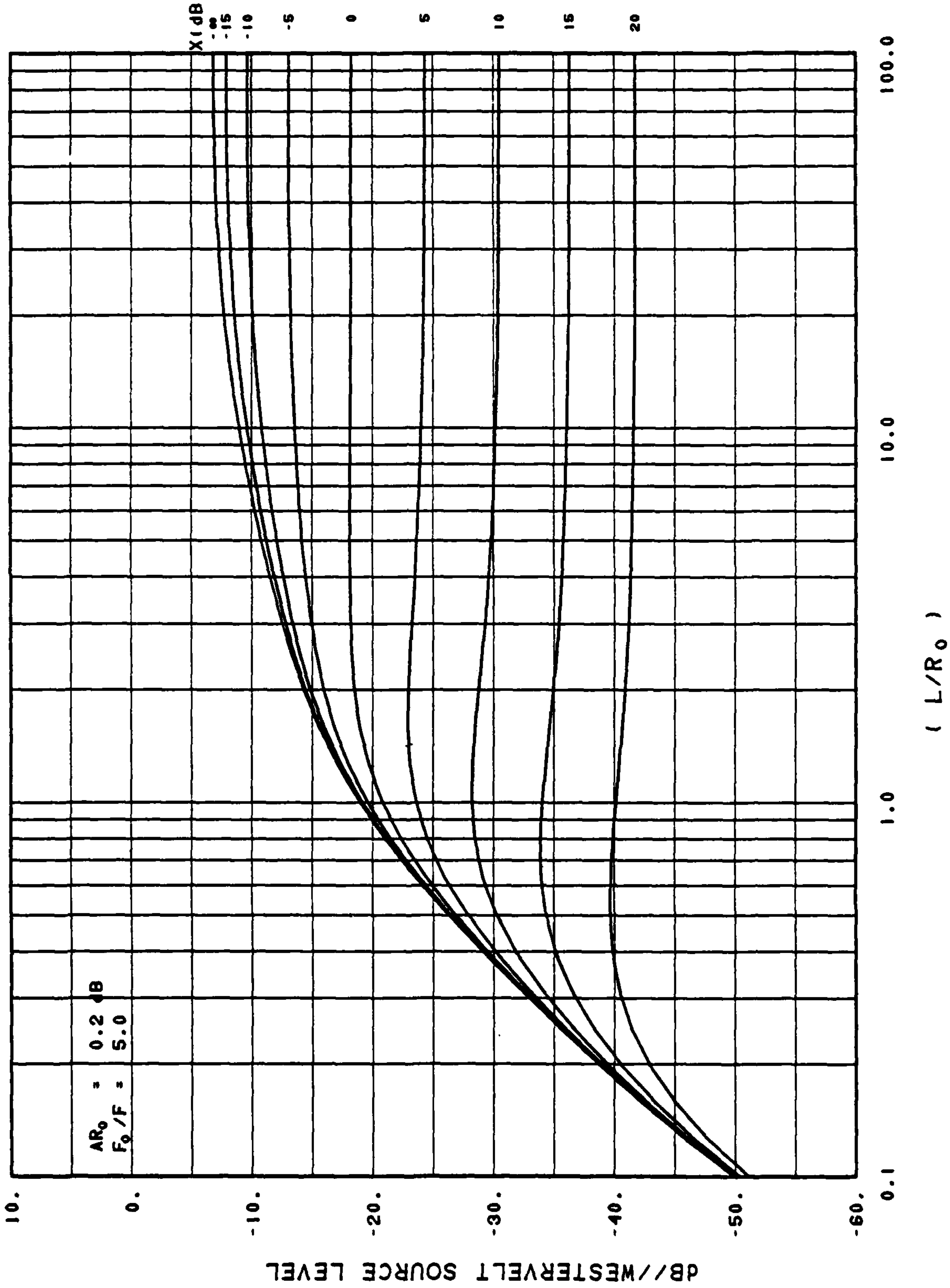

RELATIVE SOURCE LEVEL VS SCALED RANGE

Figure 9

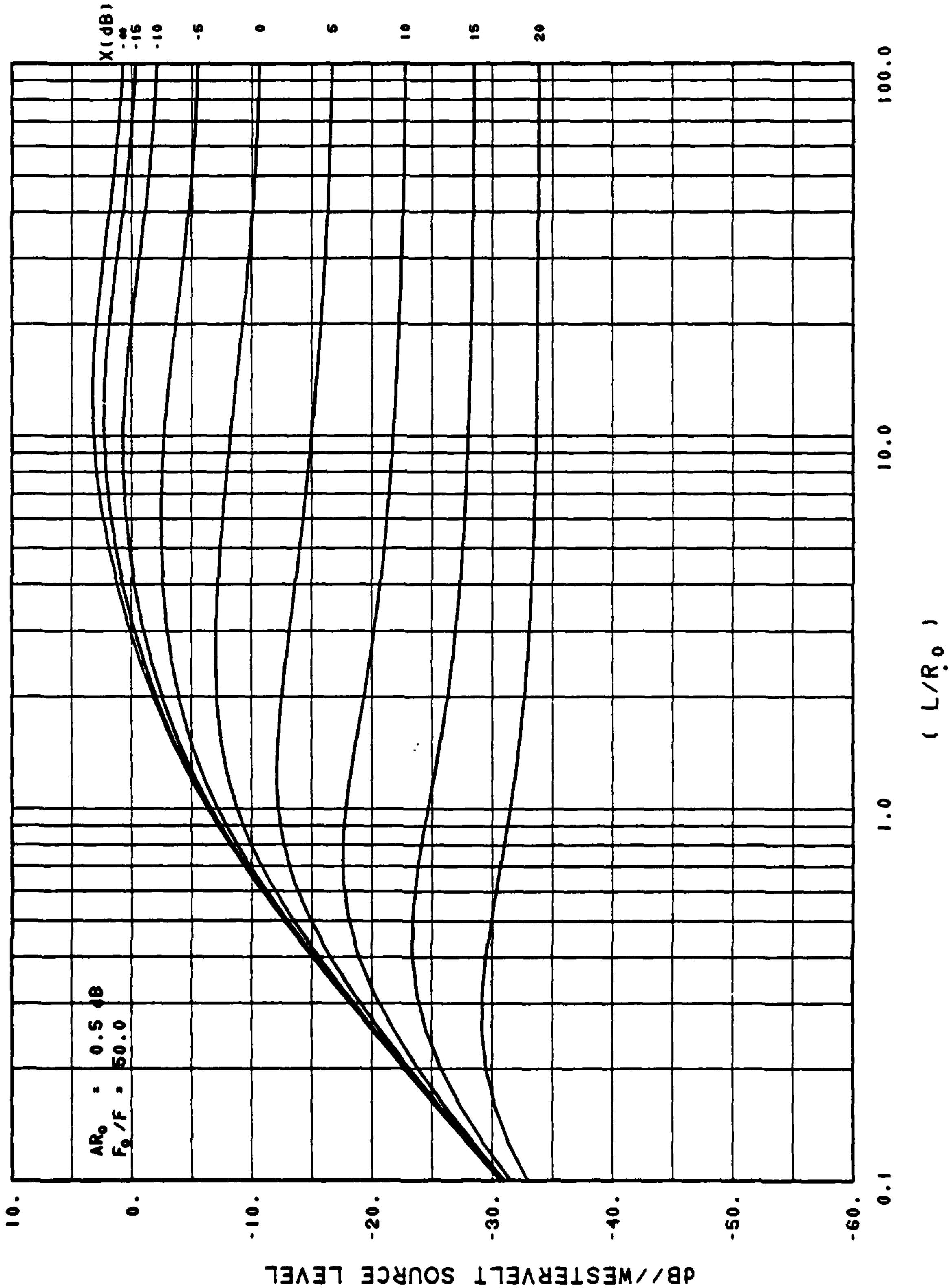

(L/R_o)

RELATIVE SOURCE LEVEL VS SCALED RANGE

Figure 10

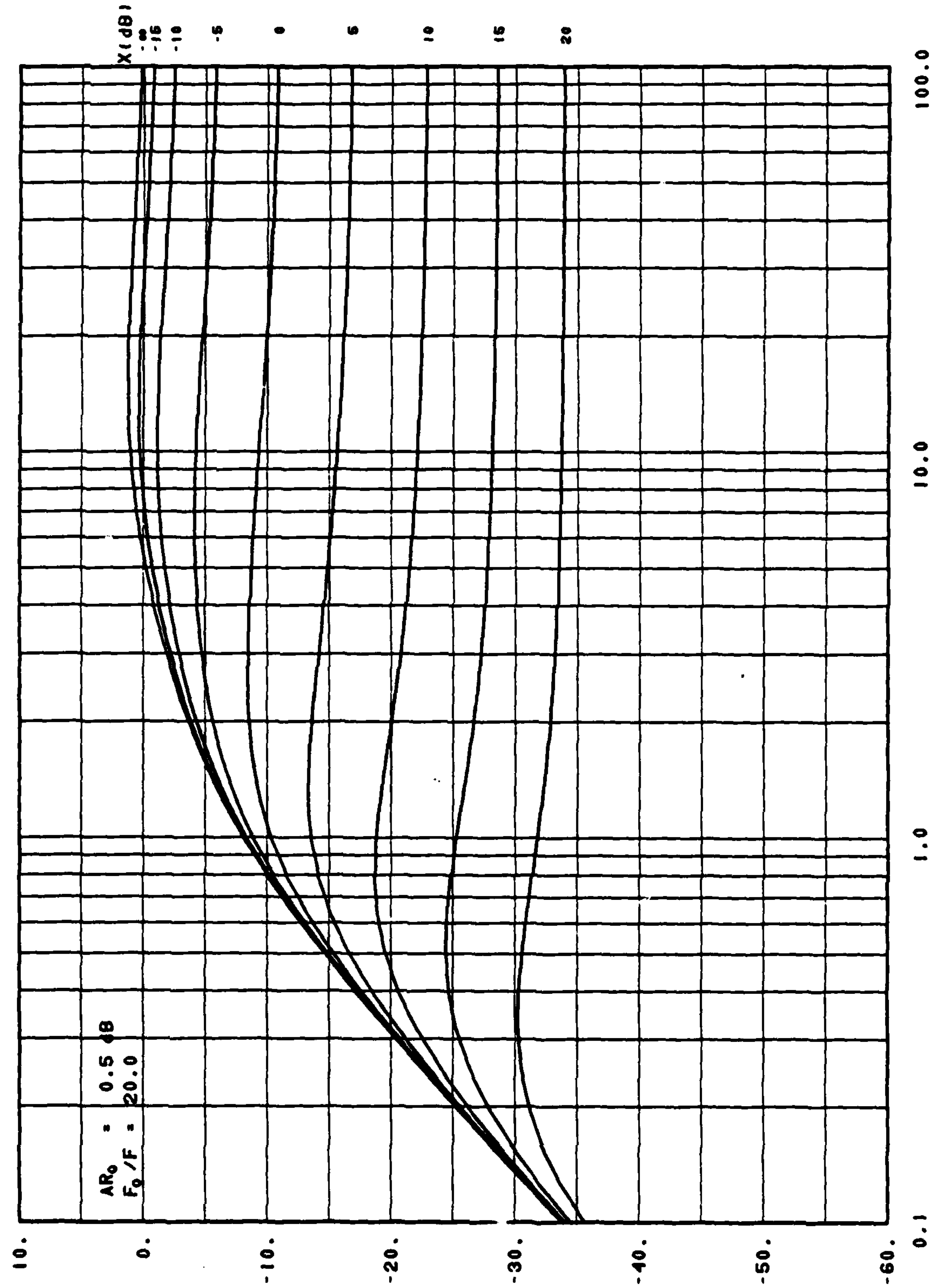

RELATIVE SOURCE LEVEL VS SCALED RANGE

Figure 11

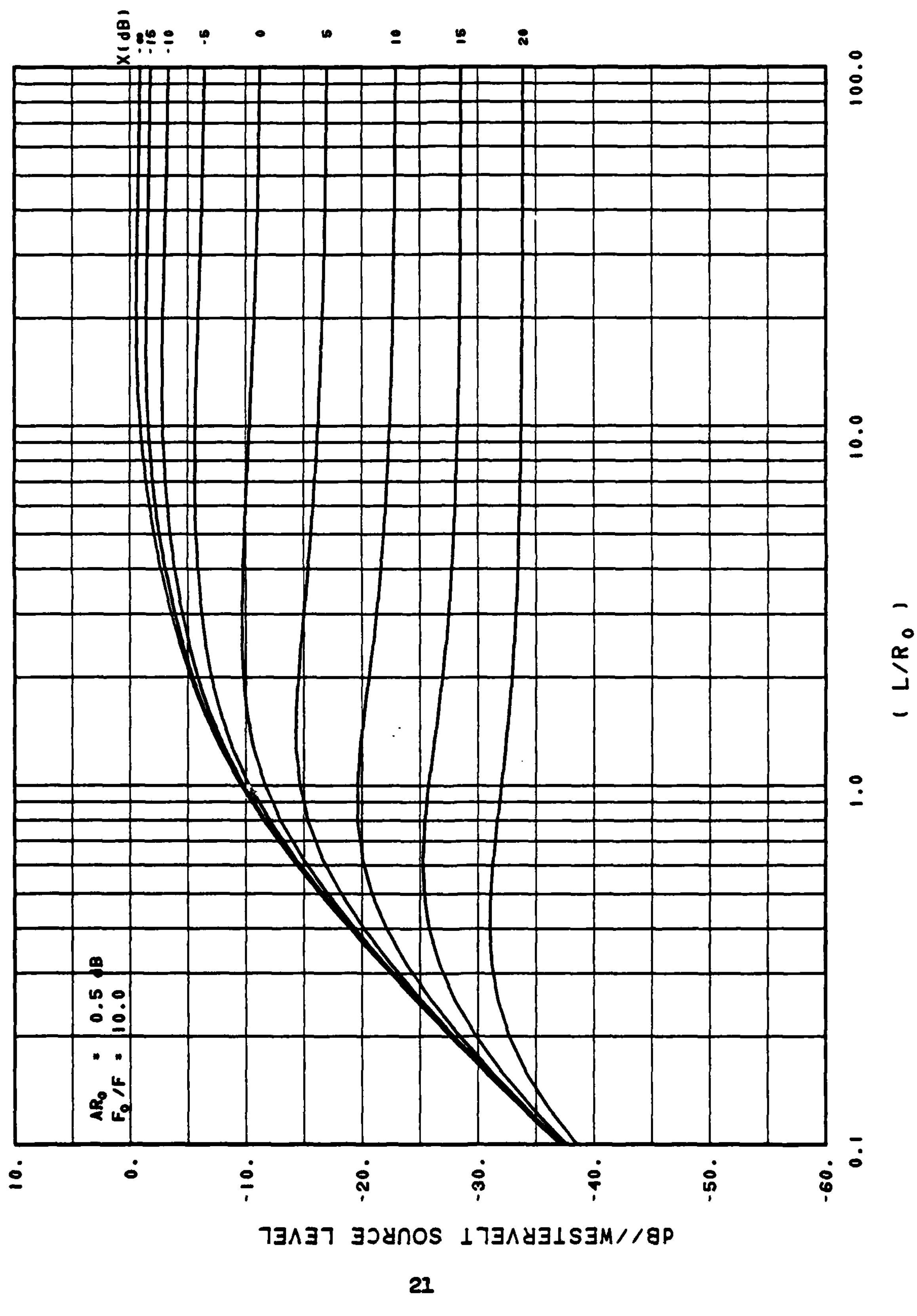

RELATIVE SOURCE LEVEL VS SCALED RANGE

Figure 12

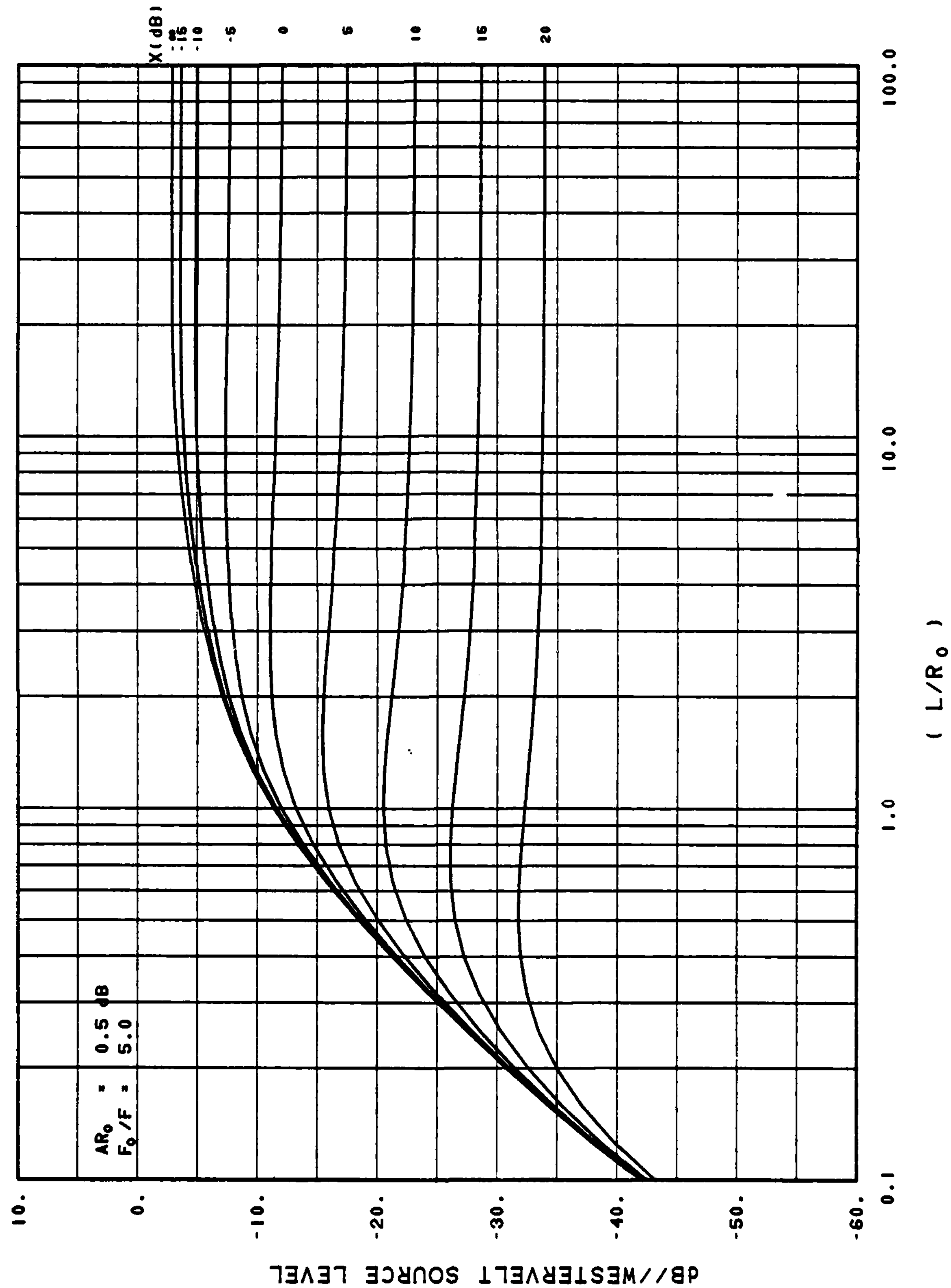

RELATIVE SOURCE LEVEL VS SCALED RANGE

Figure 13

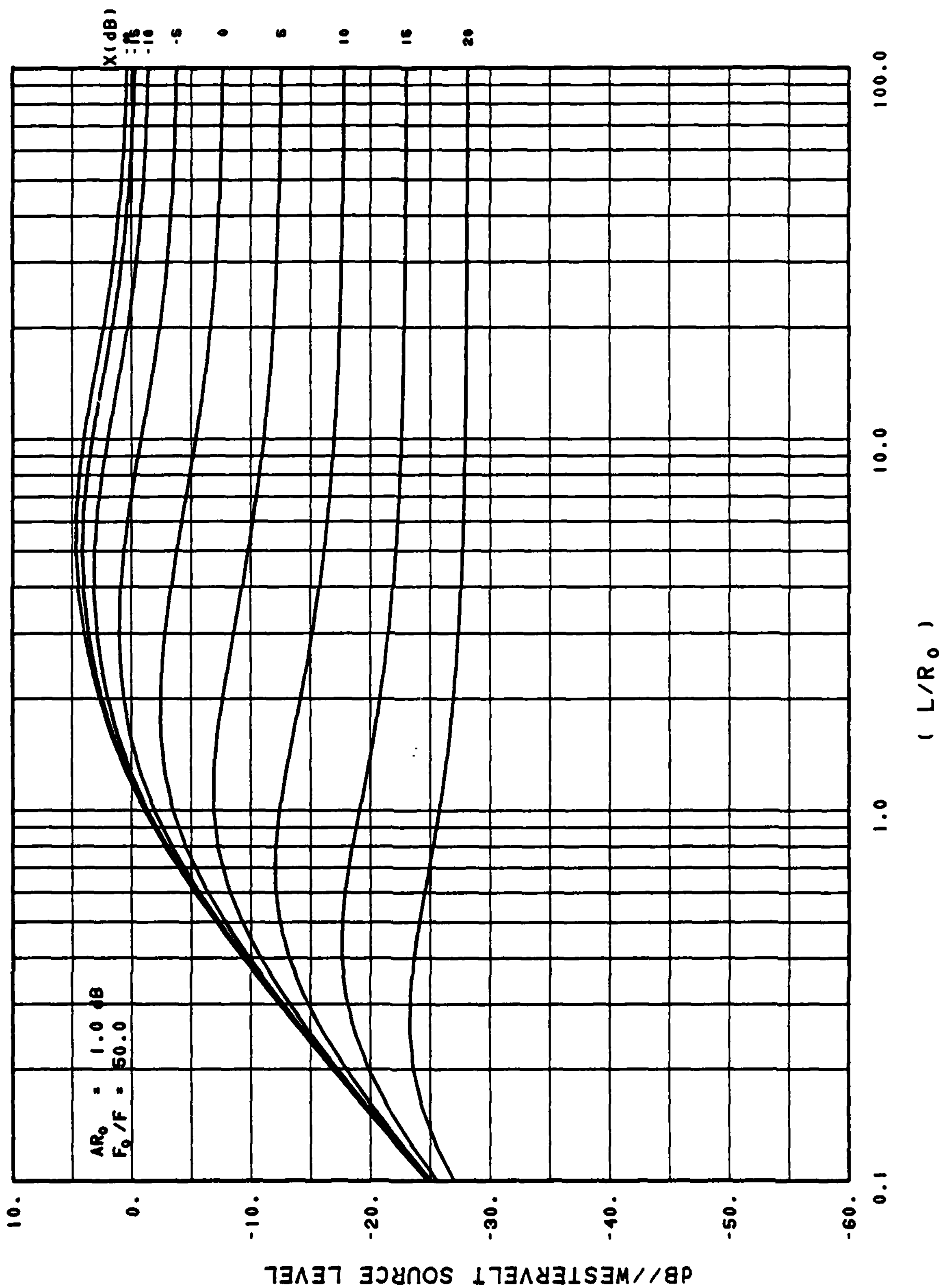

RELATIVE SOURCE LEVEL VS SCALED RANGE

Figure 14

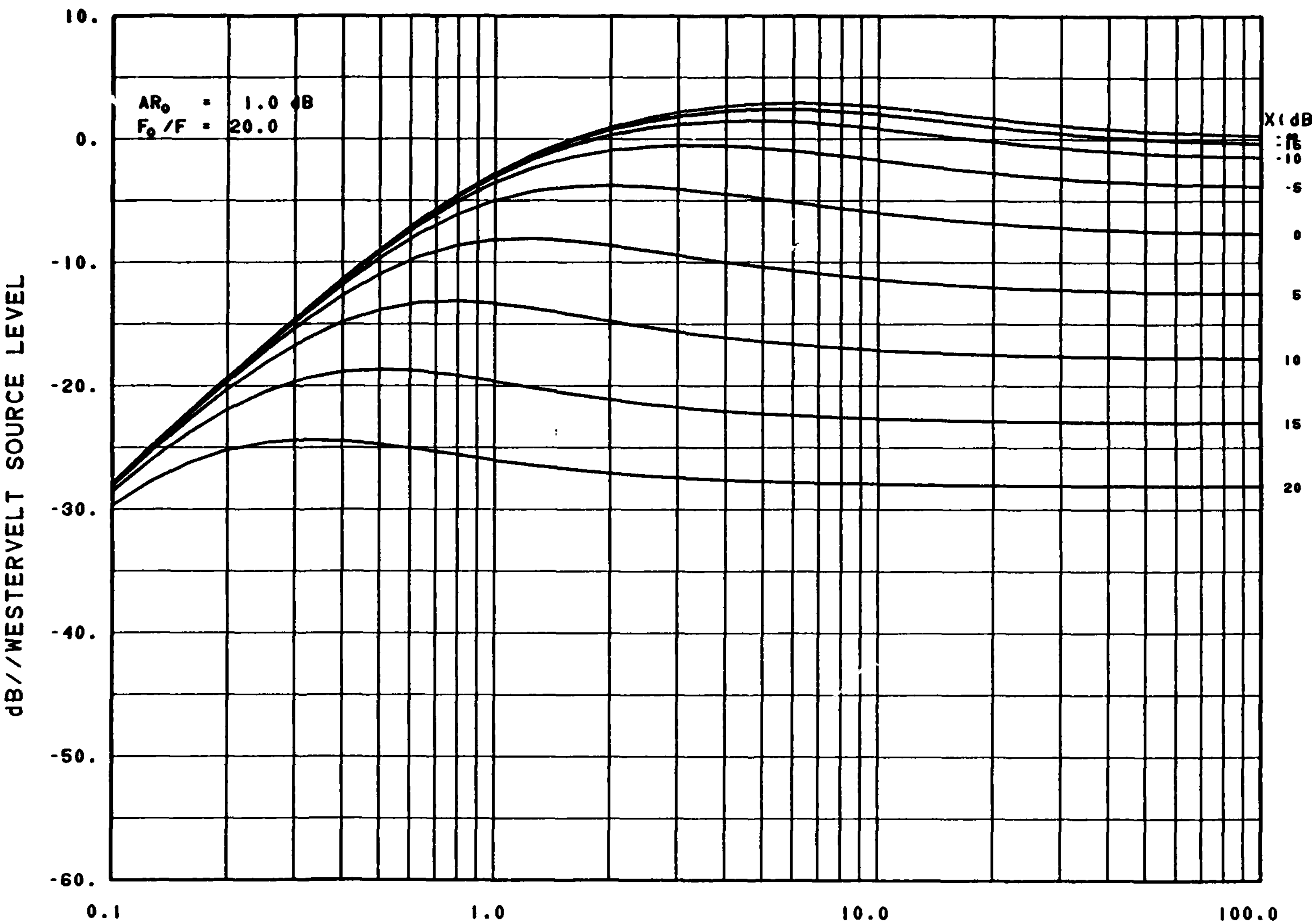

RELATIVE SOURCE LEVEL VS SCALED RANGE

Figure 15

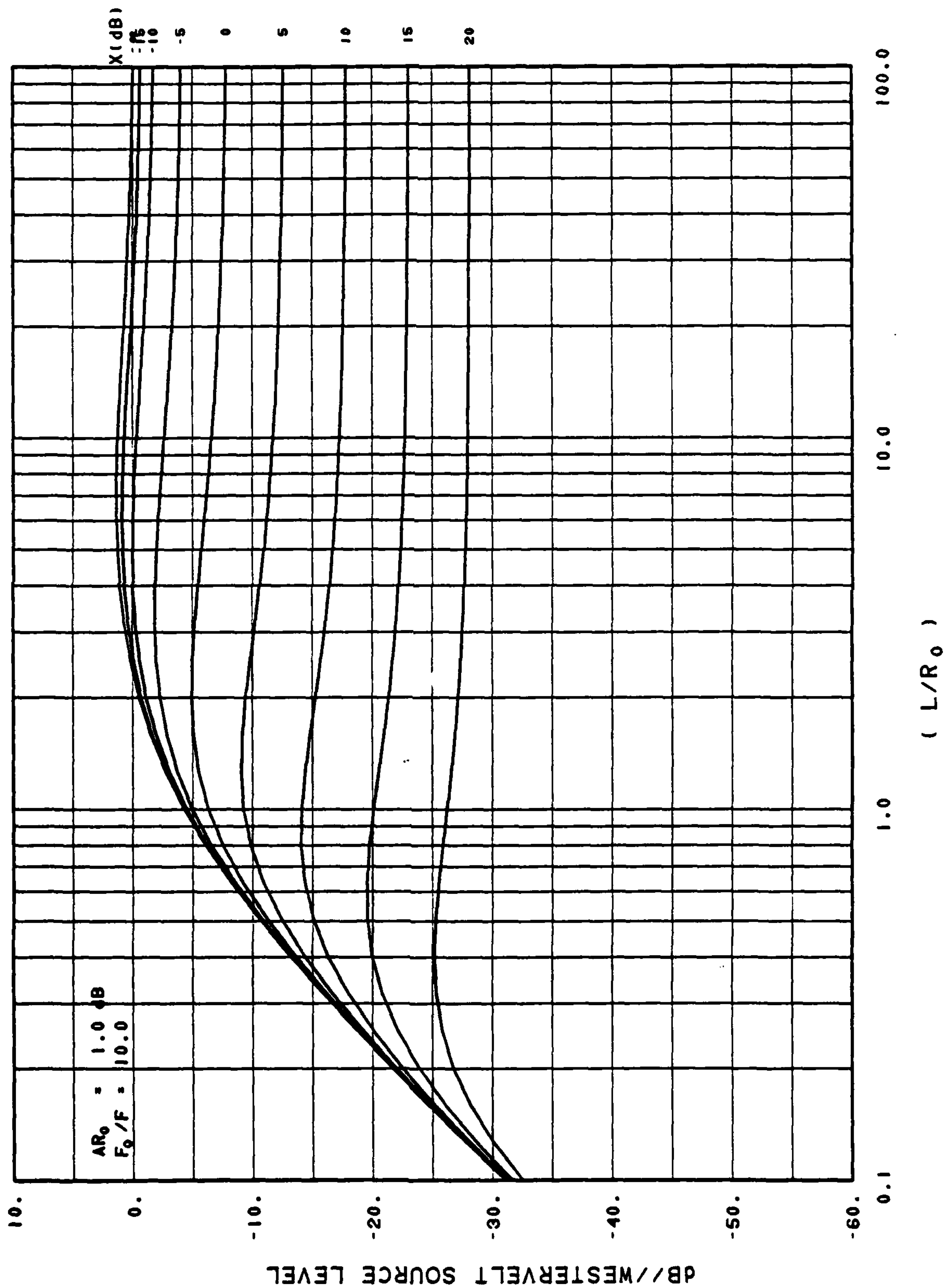

RELATIVE SOURCE LEVEL VS SCALED RANGE

Figure 16

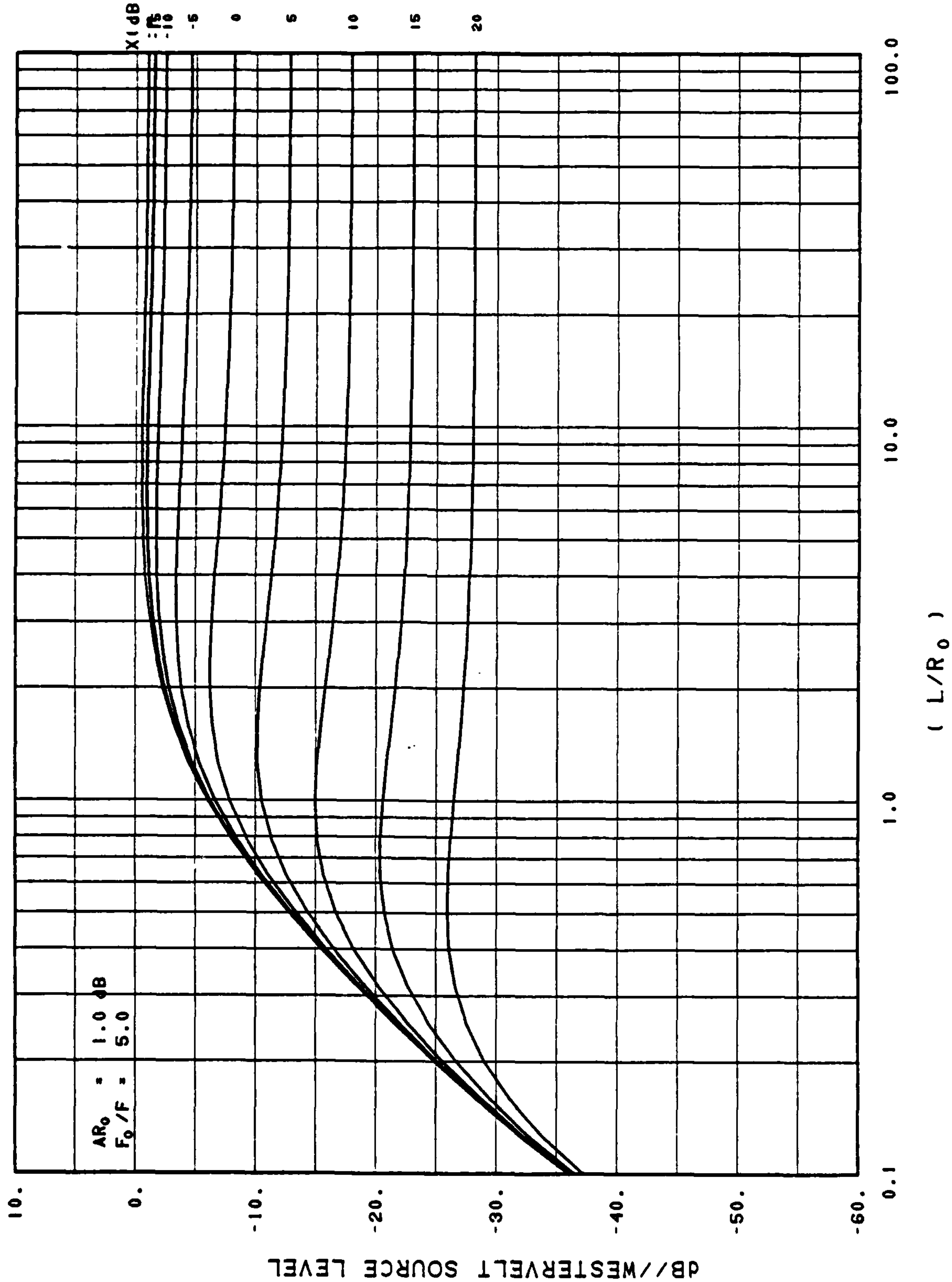

RELATIVE SOURCE LEVEL VS SCALED RANGE

Figure 17